

Photodiodes and Transimpedance Amplifiers for 100-Gbit/s Digital Coherent Optical Communications

Kimikazu Sano[†], Toshihide Yoshimatsu, Hiroyuki Fukuyama, and Yoshifumi Muramoto

Abstract

To increase transmission capacity and extend transmission distance, 100-Gbit/s digital coherent optical communications systems have been researched. NTT Photonics Laboratories has developed photodiodes that exhibit a good high-frequency response even under high optical input power and transimpedance amplifiers that have both broadband characteristics and a wide input dynamic range.

1. Introduction

To markedly increase transmission capacity and extend transmission distance, 100-Gbit/s digital coherent optical communications systems have recently been researched and developed. The architecture of optical receivers for such systems is shown in **Fig. 1**. A signal light transmitted through optical fibers (bit rate: 125.6 Gbit/s) and a local light (continuous wave) are input to the optical receiver simultaneously. The local light is necessary in order to decode the signal light, whose signal format is dual polarization quadrature phase shift keying (DP-QPSK). Both the signal light and local light have two optical polarization components (X pol. and Y pol.). Each light is split into beams with different polarizations by polarization beam splitters. Then, the polarization-split lights are fed into 90° optical hybrids. There the signal and local lights are mixed, and two optical-phase-multiplexed components (I and Q, which denote in-phase and quadrature, respectively) in the signal light are separated. The outputs of the 90° optical hybrids are of the differential style, so each hybrid has four outputs (I-pos., I-neg., Q-pos., and Q-neg. (pos.: positive, neg.: negative)). With the

polarization beam splitters and the 90° optical hybrids, the signal light, which is both optical polarization multiplexed and optical phase multiplexed, is separated into four independent differential signals. Therefore, the baud rate of each of the four separated differential signals is 31.4 Gbaud, i.e., one-fourth that of the signal light.

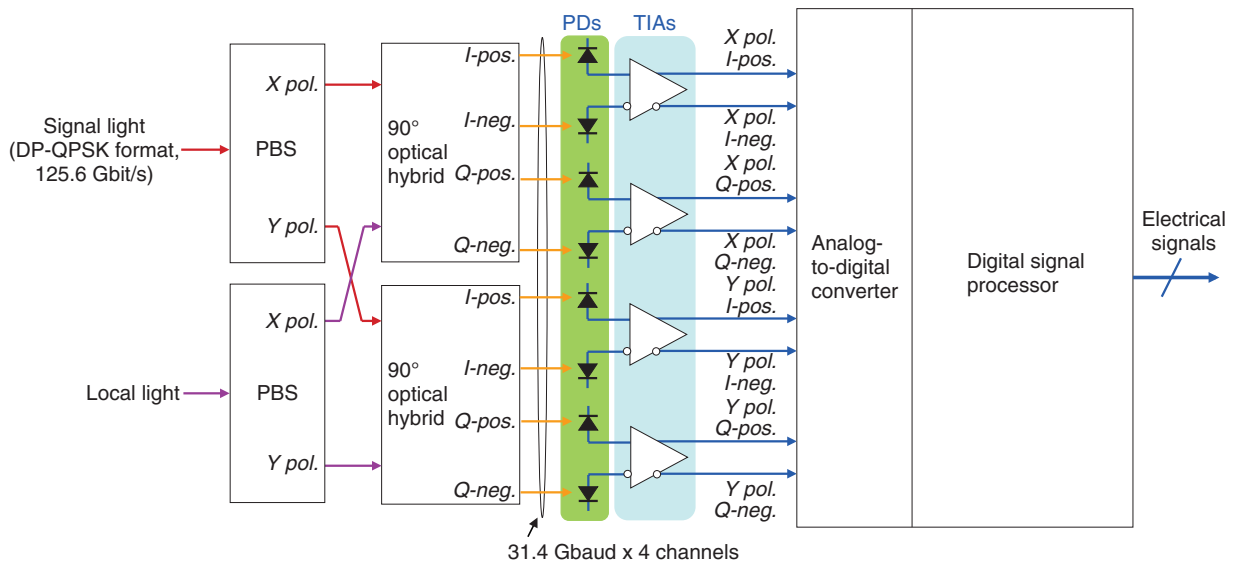
Photodiodes (PDs) convert the high-speed (31.4-Gbaud) optical signals into electrical current ones. To convert four differential optical signals, eight PDs are installed in the optical receiver.

Transimpedance amplifiers (TIAs) transform the high-speed electrical current signals into electrical voltage ones, and they linearly amplify the signals to output a constant voltage amplitude that the following analog-to-digital converters can handle. To transform and amplify four differential electrical signals independently, four TIAs are used in the optical receiver.

2. PDs for 100-Gbit/s digital coherent optical communications systems

In 100-Gbit/s digital coherent optical communication systems, high-power local light is used as one of the inputs for the optical receiver. Therefore, PDs that exhibit a good high-frequency response even under high optical input power are required. To meet this

[†] NTT Photonics Laboratories
Atsugi-shi, 243-0198 Japan



PBS: polarization beam splitter

Fig. 1. Architecture of optical receiver for 100-Gbit/s digital coherent optical communications.

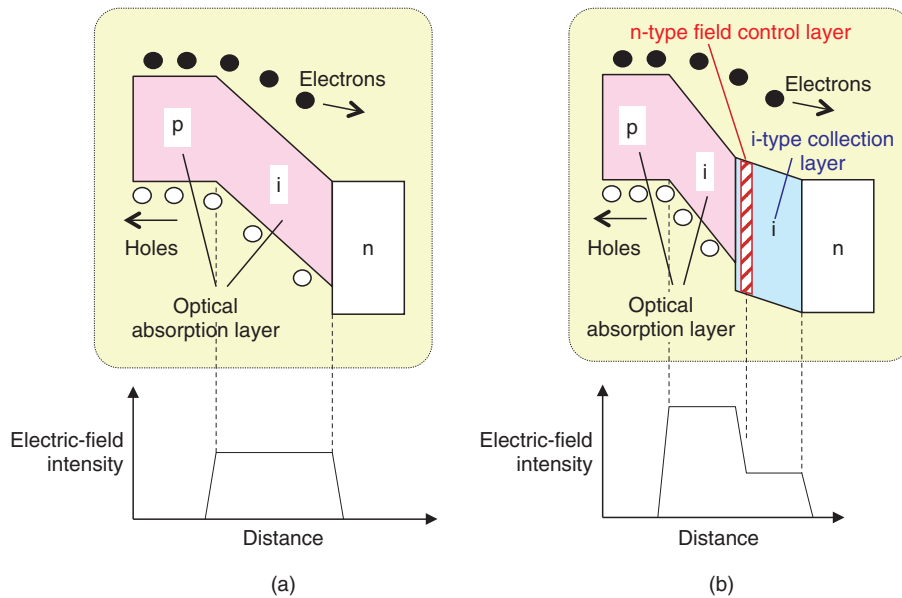


Fig. 2. Energy band diagrams for (a) conventional MIC-PD and (b) composite-field MIC-PD.

requirement, we have developed a new type of PD called a composite-field maximized-induced-current PD (composite-field MIC-PD) [1]. The energy band diagrams for the conventional MIC-PD and the composite-field MIC-PD are compared in Fig. 2. In the case of the conventional MIC-PD, under high optical

input power, the many holes that accumulate in the intrinsic (i-type) optical absorption layer weaken the electrical field and degrade the high-frequency responses of holes and electrons. This effect is known as the space charge effect. In the composite-field MIC-PD, to mitigate the space charge effect, a

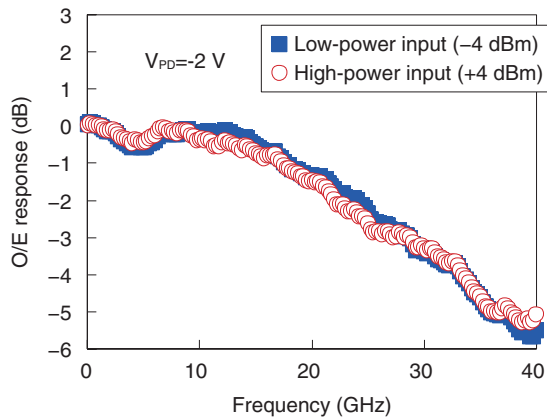


Fig. 3. Frequency optical-to-electrical (O/E) responses for a fabricated composite-field MIC-PD under optical input power of -4 dBm (low-power input) and +4 dBm (high-power input).

negative (n-type) field control layer and an i-type wide bandgap collection layer are newly introduced. These layers strengthen the electrical field of the i-type optical absorption layer and lead to improved high-frequency responses of holes and electrons under high optical input power.

Measured frequency responses for a fabricated composite-field MIC-PD under optical input power of -4 dBm (low-power input) and +4 dBm (high-power input) are shown in **Fig. 3**. For both inputs, the frequency responses are almost the same. The -3-dB-down frequencies for both inputs are 29 GHz. This result demonstrates that the composite-field MIC-PD relaxes the space charge effect and exhibits good high-frequency responses even under high optical input power.

The measured bias voltage dependences of the -3-dB-down frequencies of the composite-field and conventional MIC-PDs are compared in **Fig. 4**. In the measurement, the photocurrent value was set to 2 mA, which is close to real photocurrent values in 100-Gbit/s systems. While the conventional MIC-PD requires a bias voltage of -3.5 V for a 24-GHz -3-dB-down frequency, the composite-field MIC-PD achieves a 29-GHz -3-dB-down frequency with only a -2-V bias voltage. This shows that the electrical field of the i-type optical absorption layer is sufficiently strengthened with a bias voltage as low as -2 V. The responsivity of the composite-field MIC-PD is around 0.8 A/W, which is also high enough for 100-Gbit/s systems.

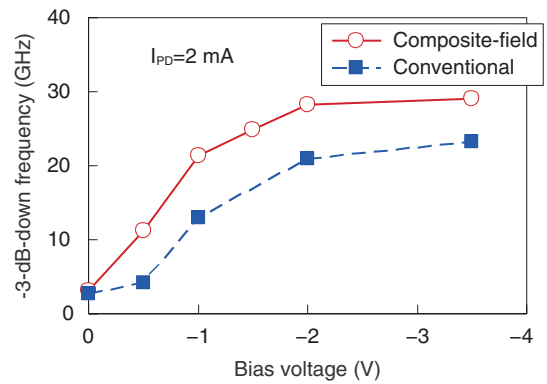


Fig. 4. Bias voltage dependencies of -3-dB-down frequencies for the composite-field MIC-PD and conventional MIC-PD.

3. TIAs for 100-Gbit/s digital coherent optical communications systems

In 100-Gbit/s digital coherent optical communications systems, TIAs need to amplify high-speed electrical signals of 31.4 Gbaud. It is empirically known that amplification of a B-baud signal needs bandwidth of $0.7B$ Hz, where B denotes the baud value. Therefore, TIAs require a broad bandwidth of $31.4 \text{ Gbaud} \times 0.7 = 22 \text{ GHz}$. In addition to the broad bandwidth, TIAs must maintain a constant voltage amplitude in a wide input current range of $\sim 100 \mu\text{A}$ to $\sim 1 \text{ mA}$.

In designing a TIA that could satisfy the above requirements, we used InP heterojunction bipolar transistors (HBTs) with a $1\text{-}\mu\text{m}$ -wide emitter. Since these InP HBTs exhibit high-frequency characteristics represented by a high current cut-off frequency (f_T) of 170 GHz, they are suitable for designing a TIA with a broad bandwidth of over 22 GHz.

The circuit diagram of the TIA that we designed is shown in **Fig. 5**. Photocurrent from the PDs is fed into the TIA's input differential terminals IT and IC. Then, the signal is amplified by the following circuit blocks: TIA core, post amplifier, variable gain amplifier (VGA), high-gain broadband amplifier (HGBA), and output buffer. Finally, differential output with a constant voltage amplitude is launched from output terminals OT and OC. To make the output voltage amplitude constant in the whole range of input current, a peak detector and an auto gain control (AGC) circuit are monolithically integrated in the TIA. The peak detector and the AGC circuit compare the real output voltage amplitude of the HGBA with a target

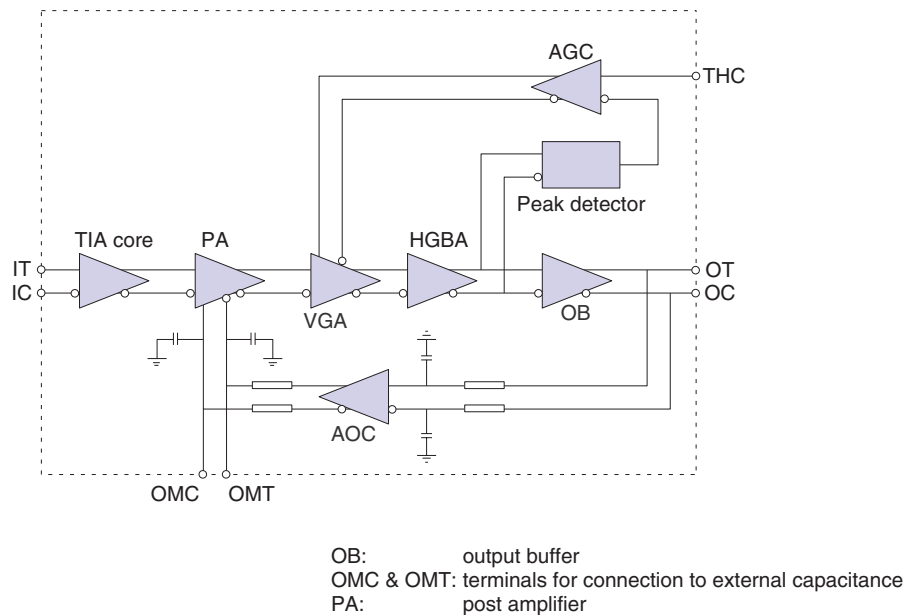


Fig. 5. Circuit diagram of the TIA.

amplitude provided through terminal THC, and they control the gain of the VGA so that the output voltage amplitude of the HGBA is equal to the target one. In this way, a function for achieving constant output voltage amplitude is implemented in the TIA. The TIA also contains an automatic offset canceling (AOC) circuit. The AOC circuit excludes DC voltage offset inside the TIA and ensures that high-speed signals are sufficiently amplified. The power supply voltage for the TIA is -5.2 V, and power consumption of one TIA is 660 mW (2.64 W for all four).

To make the output voltage amplitude constant over the whole range of input current, the VGA gain is controlled by the AGC circuit. Therefore, a variable range of VGA gain is also a key specification for keeping the output voltage amplitude constant, and it should be large enough to correspond to a wide input current range. The circuit configuration of the VGA is shown in Fig. 6(a). The VGA gain is varied by changing current IS1: the gain increases (decreases) with increasing (decreasing) IS1. The simulated frequency-gain characteristics of the VGA for minimum and maximum current IS1 are shown in Fig 6(b). While a large variable range of the gain is achieved at low frequencies, the range is reduced in the high-frequency region because of the increase in minimum gain. This is mainly due to the base-collector capacitances (C_{bc}) of transistors Q11 and Q12 (Fig. 6(a)), which bypass the high-frequency signal from input to

output. To suppress the increase in minimum gain due to C_{bc} , we added transistors Q21 and Q22 to the VGA. In the circuit configuration in Fig. 6(a), the base-collector capacitances (C_{bc}) of Q21 and Q22 cancel C_{bc} and suppress the increase in minimum gain. As a result, the variable range of the gain is widened by about 10 dB in the high-frequency region.

The frequency response of transimpedance gain for a fabricated TIA is shown in Fig. 7. Transimpedance gain at low frequency is 68 dB Ω (2510 Ω), and the -3-dB-down frequency is 23 GHz, which exceeds the value required for 100-Gbit/s systems (22 GHz).

The input current dependence of the differential output voltage amplitude for the fabricated TIA is shown in Fig. 8. Constant output voltage amplitude of 540 mVppd (ppd: peak-to-peak, differential) was confirmed for a wide input current range from 160 μ App to 2.6 mApp. This result shows that the integrated peak detector and AGC circuit successfully controlled the output amplitude to keep it constant. Furthermore, the variable range of the VGA gain was sufficient to keep a constant output amplitude. The inset of Fig. 8 shows a 32-Gbaud output eye-pattern for 260- μ App input. A clear output eye-pattern was observed for the 32-Gbaud input, which is close to the baud rate for practical 100-Gbit/s systems (31.4 Gbaud).

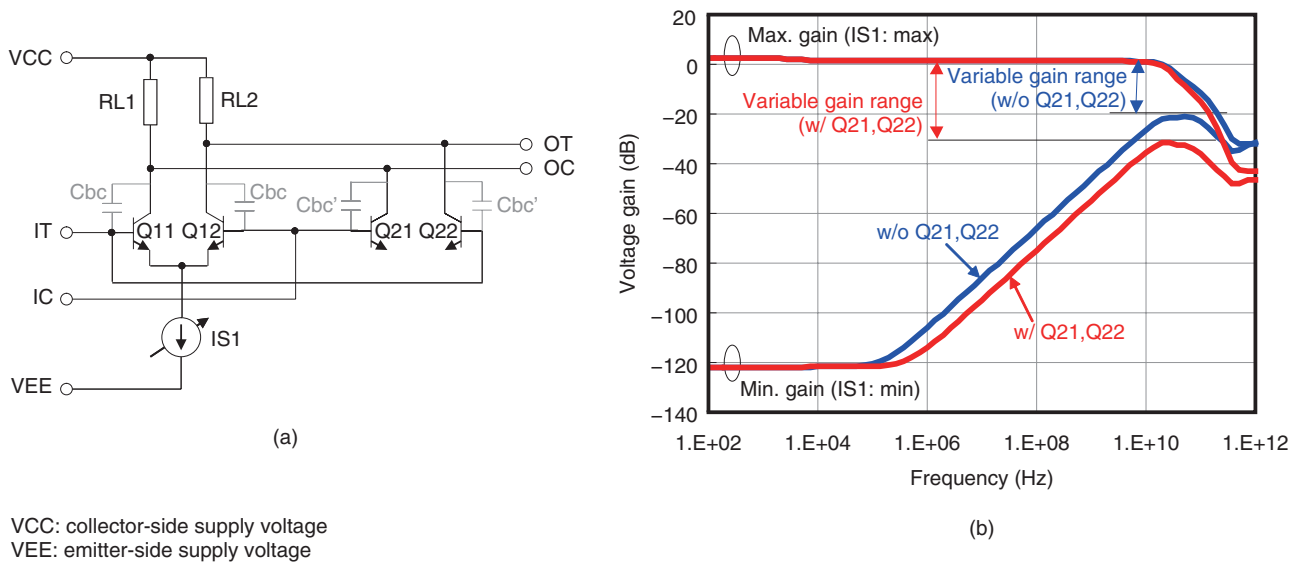


Fig. 6. (a) Circuit configuration of VGA and (b) frequency-gain characteristics of VGA (simulated).

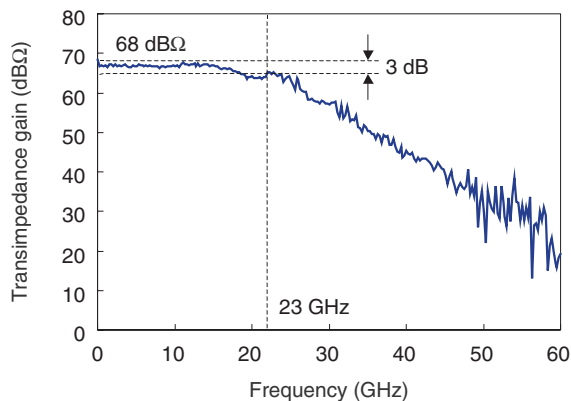


Fig. 7. Frequency response of transimpedance gain for the fabricated TIA.

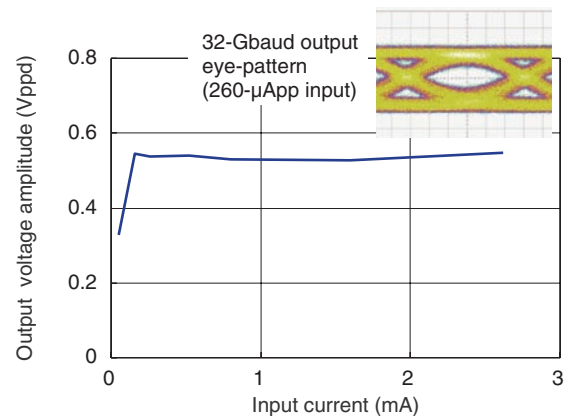


Fig. 8. Input current dependence of differential output voltage amplitude for the fabricated TIA.

4. Conclusion

We described high-speed photodiodes and transimpedance amplifiers for 100-Gbit/s digital coherent optical communications systems. For the photodiodes, we have newly devised composite-field maximized-induced-current photodiodes and confirmed their good high-frequency responses under high optical input power conditions, which are the characteristics required for 100-Gbit/s systems. We designed and fabricated the transimpedance amplifiers using InP HBTs with a 1-μm-wide emitter and confirmed a

broad bandwidth of over 22 GHz and constant output amplitude in a wide input current range. These characteristics are indispensable for 100-Gbit/s systems.

In the future, we will research and develop photodiodes that can handle much higher optical input power and transimpedance amplifiers that can keep a constant output amplitude in wider input current ranges.

Acknowledgment

This work was partly supported by the Ministry of Internal Affairs and Communications (MIC) of Japan

through the R&D project “High-speed Optical Transport System Technologies”.

Reference

- [1] T. Yoshimatsu, Y. Muramoto, S. Kodama, T. Furuta, N. Shigekawa, H. Yokoyama, and T. Ishibashi, “Composite-field MIC-PDs for Low-bias-voltage Operation,” Proc of the 22nd International Conference on Indium Phosphide and Related Materials, pp. 417–420, Kagawa, Japan, 2010.



Kimikazu Sano

Senior Research Engineer, High-speed Devices and Technology Laboratory, NTT Photonics Laboratories.

He received the B.S., M.S., and Ph.D. degrees in electrical engineering from Waseda University, Tokyo, in 1994, 1996, and 2004, respectively. He joined NTT Laboratories in 1996. Since then, he has worked on the design of ultrafast digital and analog ICs/OEICs using GaAs MESFETs, InP-based HEMTs, InP-based HBTs, InP-based tunneling diodes, and InP-based photodiodes. From 2005 to 2006, he was a visiting researcher at the University of California, Los Angeles (UCLA), where he researched a microwave/millimeter sensing system. He received the Young Researcher's Award from the International Conference on Solid State Devices and Materials (SSDM) in 2003. He is a member of IEEE and the Institute of Electronics, Information and Communication Engineers (IEICE).



Toshihide Yoshimatsu

Research Engineer, High-speed Devices and Technology Laboratory, NTT Photonics Laboratories.

He received the B.E. and M.E. degrees in applied physics from Tohoku University, Miyagi, in 1998 and 2000, respectively. He joined NTT Photonics Laboratories in 2000. He has been engaged in research on ultrafast opto-electronic devices. He received the SSDM Paper Award from SSDM in 2004. He is a member of IEICE and the Japan Society of Applied Physics (JSAP).



Hiroyuki Fukuyama

Senior Research Engineer, High-speed Devices and Technology Laboratory, NTT Photonics Laboratories.

He received the B.S. and M.S. degrees in physics from Keio University, Kanagawa, in 1988 and 1990, respectively. In 1990, he joined NTT LSI Laboratories, Kanagawa, where he engaged in research on resonant tunneling devices and their microwave applications. He is currently engaged in research on high-speed devices and circuit design for optical communications systems.



Yoshifumi Muramoto

Senior Research Engineer, High-speed Devices and Technology Laboratory, NTT Photonics Laboratories.

He received the B.E. and M.E. degrees from Osaka Prefecture University in 1990 and 1992, respectively. He joined NTT Laboratories in 1992. He has been engaged in research on monolithically integrated photoreceivers and high-speed photodetectors. He is a member of IEICE and JASP.